

Metal-insulator transition in a two-dimensional system of chiral unitary classJonas F. Karcher ^{1,2,3} Ilya A. Gruzberg ⁴ and Alexander D. Mirlin ^{2,3}¹*Department of Physics, Pennsylvania State University, University Park, Pennsylvania 16802, USA*²*Institute for Quantum Materials and Technologies, Karlsruhe Institute of Technology, 76021 Karlsruhe, Germany*³*Institut für Theorie der Kondensierten Materie, Karlsruhe Institute of Technology, 76128 Karlsruhe, Germany*⁴*Department of Physics, Ohio State University, 191 West Woodruff Avenue, Columbus Ohio, 43210, USA*

(Received 6 October 2022; accepted 11 January 2023; published 27 January 2023)

We perform a numerical investigation of Anderson metal-insulator transition (MIT) in a two-dimensional system of chiral symmetry class AIII by combining finite-size scaling, transport, density of states, and multifractality studies. The results are in agreement with the σ -model renormalization-group theory where MIT is driven by proliferation of vortices. We determine the phase diagram and find an apparent nonuniversality of several parameters on the critical line of MIT, which is consistent with the analytically predicted slow renormalization towards the ultimate fixed point of the MIT. The localization-length exponent ν is estimated as $\nu = 1.55 \pm 0.1$.

DOI: [10.1103/PhysRevB.107.L020201](https://doi.org/10.1103/PhysRevB.107.L020201)

Introduction. Anderson transitions (ATs) in disordered systems—which include metal-insulator transitions (MITs) as well as transitions between topologically distinct insulating phases—remain a dynamic field of research [1]. In this context, two-dimensional (2D) systems attract particular attention. On the experimental side, there is a variety of realizations of 2D electronic disordered systems, including semiconductor heterostructures, graphene, and other 2D materials, oxide heterostructures, as well as surfaces of topological insulators and superconductors. Furthermore, investigation of 2D-disordered systems in photonic structures is an emerging research area [2].

For the most conventional setting of a quantum particle in a random potential (Wigner-Dyson orthogonal symmetry class AI), $d = 2$ is a lower critical dimensionality as for conventional second-order phase transitions with continuous symmetry. This implies that there is no AT in 2D systems of this symmetry class, and all states are localized (although the localization length is exponentially large for weak disorder). At the same time, it was realized that there is a number of mechanisms generating ATs in 2D-disordered systems of other symmetry classes. Although field theories of ATs are nonlinear σ models with a continuous non-Abelian symmetry, the existence of metallic (symmetry-broken) phases in 2D geometry is not in conflict with the Mermin-Wagner theorem, in view of an unconventional character of the symmetry groups (involving supersymmetry and noncompactness or replica limit, depending on the formulation).

The 2D ATs include, in particular, MITs in classes AII, D, and DIII with broken spin-rotation invariance playing a crucial role as well as quantum-Hall transitions in classes A, C, and D that are governed by topology. Whereas ATs of these types have been studied in a rather detailed fashion, there is one more type of 2D ATs that has received much less attention: MITs in chiral classes AIII, BDI, and CII. In fact, early studies demonstrated a resilience of chiral systems to

Anderson localization, leading to a suggestion that 2D and three-dimensional (3D) systems of chiral symmetry classes do not exhibit AT at all, remaining always in a delocalized phase [3]. This has received an apparent support from the renormalization-group (RG) analysis of the corresponding σ models performed in pioneering works of Gade and Wegner [4] and Gade [5], which yielded no quantum corrections to conductivity (and, thus, no localization) to all orders in perturbation theory. The Gade-Wegner RG implies that 2D systems of chiral classes possess a metallic phase with a line of infrared-stable fixed points with different values of conductivity. The special character of RG in chiral classes is related to the fact that the corresponding σ -model manifolds contain an additional $U(1)$ degree of freedom.

More recently, numerical studies of suitably designed 2D models of chiral classes have provided evidence of Anderson MITs [6,7]. An analytical theory of 2D ATs in chiral classes was developed in Ref. [8]. It was pointed out in Ref. [8] that, since the σ -model manifolds for chiral classes are not simply connected [due to the $U(1)$ degree of freedom], they allow for topological excitations—vortices. Inclusion of the vortices in the RG analysis leads to a metal-insulator phase transition [8], in an analogy with the famous Berezinskii-Kosterlitz-Thouless (BKT) transition in the XY model. The analysis of the resulting RG flow showed, however, that there is an essential difference: The transition happens at a finite fugacity $y > 0$ at variance with the fixed point value $y = 0$ for the BKT transition. This hinders a fully controllable analytical calculation of critical exponents at MITs in chiral classes, thus, making numerical studies of these transitions even more important. The central goal of this paper is a numerical study of the 2D MIT in the chiral unitary class AIII.

Chiral classes. The special character of disordered systems of chiral symmetry classes has been understood since the pioneering work of Dyson who found a singularity of the density of states in one-dimensional (1D) harmonic chains at zero

energy (chiral symmetry point) [9]. Further works extended the analysis to localization properties and to quasi-1D systems. It was found that an N -channel quasi-1D system of the chiral class has N topological phases. At transitions between these phases, the density of states exhibits the Dyson singularity [10,11], and the localization length diverges [12–20]. Critical points of these transitions have infinite-randomness character with critical wave functions showing very strong fluctuations [15,21].

For 2D chiral-class systems, most of the past research focused on properties of the metallic phase. The Gade-Wegner σ model was re-derived and analyzed in many works [22–25]. Particular attention was paid to the asymptotic infrared behavior, which is of infinite-randomness character, exhibiting a very strong divergence of the density of states and a “freezing” of the multifractality spectrum [6,26–28]. On the numerical side, most papers showed critical properties of the metallic phase that are characterized by nonuniversal exponents for various observables (such as multifractality, density of states, and localization length at finite energy) [29–34] and are essentially different from those expected in the infinite-randomness infrared limit. This is not surprising: the Gade-Wegner flow towards the line of infrared fixed points is logarithmically slow so that in a typical situation the infrared limiting behavior can likely be out of reach on any realistic length scale. In several works [35–37], evidence of the asymptotic behavior of the lowest Lyapunov exponents in the quasi-1D geometry has been reported.

Apart from realizations in disordered electronic systems, the interest to models in the chiral classes is due to their relation to models of Dirac fermions coupled to fluctuating gauge fields that are discussed in the context of quantum chromodynamics (QCD) [38]. It was proposed that ATs in such models may be connected to QCD phase transitions [39]. It is also worth mentioning that chiral-class models can be experimentally realized in microwave setups based on coupled resonators [40]. Recently, MITs in 3D chiral-class systems were studied in Refs. [41,42]. Furthermore, chiral models are closely related [43–45] to non-Hermitian Anderson transitions attracting much interest [45–48].

Field theory of 2D chiral AT. In the fermionic replica formalism, the σ -model manifolds for classes AIII, BDI, and CII are $U(n)$, $U(2n)/\text{Sp}(2n)$, and $U(n)/O(n)$, respectively. In the analytical and numerical analysis below, we focus on the class AIII. The Gade-Wegner σ -model action has the form [4,5]

$$S[Q] = - \int d^2r \left[\frac{\sigma}{8\pi} \text{Tr}(U^{-1} \nabla U)^2 + \frac{\kappa}{8\pi} (\text{Tr} U^{-1} \nabla U)^2 \right].$$

Here $U(\mathbf{r}) \in U(n)$ (with the replica limit $n \rightarrow 0$ to be taken at the end of the calculation), σ is the conductivity in units of $e^2/\pi h$; the second term (known as “the Gade term”) couples only to the $U(1)$ degree of freedom and is specific for chiral classes. To describe the transition, one has to include also vortices with a fugacity y [8]. The RG equations for three couplings σ , κ , and y read

$$\partial K / \partial \ln L = 1/4 - 2Ky^2, \quad (1)$$

$$\partial y / \partial \ln L = (2 - K)y, \quad (2)$$

$$\partial \sigma / \partial \ln L = -\sigma y^2, \quad (3)$$

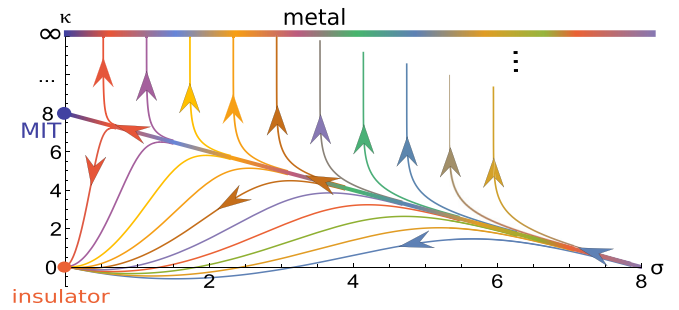


FIG. 1. Schematic of the RG flow implied by Eqs. (1)–(3). The starting value y_0 of the fugacity is taken to be the critical one $y_0 = \frac{1}{4}$ and the resulting flow is projected to the σ - κ plane.

where $K = (\sigma + \kappa)/4$. Equations (1) and (2) form a closed system with a fixed point at $K = 2$ and $y = \frac{1}{4}$. In the three-dimensional parameter space (σ, κ, y) , this corresponds to a critical line of MITs, $\sigma + \kappa = 8$, $y = \frac{1}{4}$. Along this line, there is a flow according to Eq. (3) towards the ultimate fixed point $\sigma = 0$, $\kappa = 8$, and $y = \frac{1}{4}$. This flow is, however, very slow: $\sigma(L) = \sigma_0 L^{-1/16}$. Therefore, whereas in the strict infrared limit the transition is described by the ultimate fixed point, on realistic scales one expects to see a transition described by some point on the critical line. This is expected to lead to an apparent nonuniversality of some of critical properties as discussed below.

The RG flow that follows from Eqs. (1)–(3) is illustrated in Fig. 1. The overall flow is three dimensional and is, thus, difficult to display. What is shown is the projection of the flow on the σ - κ plane with all RG trajectories having an initial value of the fugacity $y_0 = \frac{1}{4}$. The fixed points of the flow are as follows. First, there is an infrared-stable line of fixed points describing the metallic phase with σ being an arbitrary constant, $\kappa \rightarrow \infty$, $y \rightarrow 0$. Second, there is an infrared-stable fixed point describing the insulating phase: $\sigma, \kappa \rightarrow 0$ and $y \rightarrow \infty$. Finally, there is a fixed point $\sigma = 0$, $\kappa = 8$, $y = \frac{1}{4}$, describing the MIT. It has one unstable direction so that there is a two-dimensional critical surface with a flow towards this point. A cross section of this surface with the plane $y = \frac{1}{4}$ is the critical line $\sigma + \kappa = 8$ shown in Fig. 1.

Linearizing the RG Eqs. (1) and (2) near the transition point, we get the critical exponent of the localization length $\nu = 1.54$ and the irrelevant exponent $y_{\text{irr}} = 0.77$. In addition, there is a very slow flow towards the fixed point along the critical line described by Eq. (3); it yields an exponent $y'_{\text{irr}} = 1/16 \simeq 0.06$. The fact that the ultimate fixed point of the transition is at $\sigma = 0$ implies very strong fluctuations of critical eigenfunctions in the infrared limit (with freezing of the multifractal spectrum). This is expected on physical grounds: we know that eigenstates in the metallic phase possess this property, and it would be surprising if eigenstates at the transition would be “less localized” than in the metal.

Let us reiterate that the RG equations are only controllable at $y \ll 1$. Since the fixed point of the transition is at $y = \frac{1}{4}$ that is not parametrically small, all quantitative conclusions about the transition should be taken with caution. A plausible assumption is that the obtained flow is qualitatively correct but numbers describing the transition may differ substantially. It

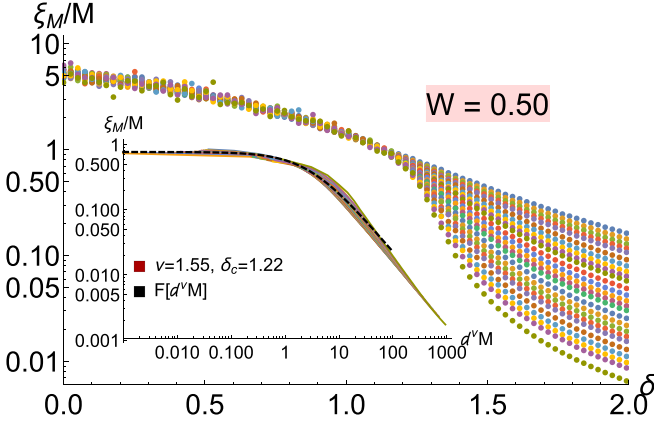


FIG. 2. Finite-size scaling analysis. Ratio ξ_M/M as a function of staggering δ for disorder $W = 0.5$ and $M = 12, \dots, 256$. The inset: data collapse $\xi_M/M = F(d^\nu M)$ with $d = \delta - \delta_c$, critical staggering $\delta_c = 1.22$, and the exponent $\nu = 1.55$.

is, thus, crucially important to explore the transition numerically, which is performed below.

Model. We study the bipartite Hamiltonian defined on a square lattice,

$$H = \sum_{i,j} [c_{i,j}^\dagger t_{i,j}^{(x)} c_{i+1,j} + c_{i,j}^\dagger t_{i,j}^{(y)} c_{i,j+1} + \text{H.c.}], \quad (4)$$

with hoppings,

$$\begin{aligned} t_{i,j}^{(x)} &= [1 + \frac{1}{2}(e^{-\delta} - 1)[(-1)^i + 1]](1 + v_{i,j}), \\ t_{i,j}^{(y)} &= [1 + \frac{1}{2}(e^{-\delta} - 1)[(-1)^j + 1]](1 + w_{i,j}). \end{aligned} \quad (5)$$

Disorder is introduced via random $v_{i,j}$ and $w_{i,j}$, whose real and imaginary parts are drawn independently from box distributions on $[-W/2, W/2]$. Since the matrix elements are complex, the time-reversal symmetry is broken, which puts H in the chiral unitary class AIII. The real parameter δ controls the degree of staggering, which is absent for $\delta = 0$ and maximal for $\delta \rightarrow \pm\infty$, when the system decouples into 2×2 plaquettes.

Finite-size scaling. To locate the MIT, we use the transfer-matrix method for a quasi-1D strip of width $M = 12, \dots, 256$ and large length $L = 10^5$ with periodic boundary conditions in the transverse (M) direction. The extracted Lyapunov exponents $\lambda_{k,M}$ become self-averaging at large L . The inverse of the smallest Lyapunov exponent yields the quasi-1D localization length $\xi_M = \lambda_{0,M}^{-1}$. In the localized phase, ξ_M is determined, for large M , by the 2D localization length ξ_{2D} so that $\xi_M/M \rightarrow 0$ at $M \rightarrow \infty$. In contrast, in the metallic phase, the large- M limit of ξ_M/M is nonzero. Note that this limit is finite (at variance with conventional MITs), which reflects a peculiar critical nature of the metallic phase in 2D chiral-class systems.

In Fig. 2, we show the ratio ξ_M/M for various M 's as a function of δ for $W = 0.5$. The plot clearly shows an MIT at $\delta_c \simeq 1.2$. The same analysis is carried out for $W = 0.3, 1.0, 2.0, 3.0$, see the Supplemental Material (SM) [49]. The resulting phase diagram is shown in Fig. 3. Applying a

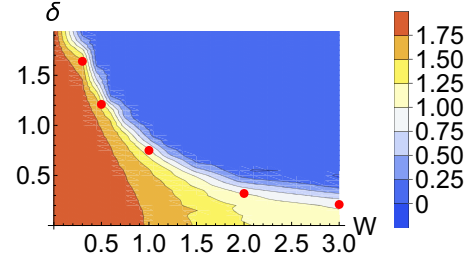


FIG. 3. Phase diagram of MIT on the (W, δ) plane. Red symbols: MIT critical values $\delta_c(W)$ obtained by transfer-matrix analysis, see Fig. 2. Color code: Inverse participation ratio (IPR) exponent, $\tau_2(L) = -\partial \ln P_2(L)/\partial \ln L$ for largest available L 's.

scaling fit (see the inset of Fig. 2), $\xi_M/M = F(d^\nu M)$ with $d = \delta - \delta_c$, we find the exponent of the localization length $\nu = 1.55 \pm 0.1$ in remarkable agreement with the value $\nu = 1.54$ obtained from the RG Eqs. (1) and (2). A very close result for ν was obtained very recently for a related non-Hermitian model [45].

Let us emphasize an apparent nonuniversality of the ratio ξ_M/M at criticality, see Table I. This is consistent with a very slow RG flow along the critical line $\sigma + \kappa = 8$ predicted analytically.

IPR. A complementary approach is to study directly properties of eigenstates $\psi(\mathbf{r})$ of a 2D system. We performed the exact diagonalization of $L \times L$ systems with $L = 24, \dots, 768$ and periodic boundary conditions, averaging over $N = 500$ disorder realizations and over all L^2 points $\mathbf{r} = (i, j)$ in the system. Detailed results for the averaged IPR $P_2 = L^2 \langle |\psi(\mathbf{r})|^4 \rangle$ of an eigenstate with the energy closest to zero are presented in the SM [49]. In the localized phase, P_2 quickly saturates when L exceeds ξ_{2D} . On the other hand, in the metallic phase, P_2 decreases with increasing L . In Fig. 3, we show by a color code the IPR exponent $\tau_2(L) = -\partial \ln P_2(L)/\partial \ln L$ calculated in the range of our largest L . A nice agreement with the phase boundary obtained from the finite-size scaling analysis is observed.

Density of states. In Fig. 4, we show the exponent $\alpha_\nu(W, \delta)$ characterizing the scaling of the density of states (DOS) $\nu(\epsilon) \propto \epsilon^{\alpha_\nu}$ across the transition for various W 's. In the metallic phase, $|\delta| < \delta_c(W)$, the RG predicts $\alpha_\nu \rightarrow -1$ at $L \rightarrow \infty$. The RG flow to this (infinite-randomness) fixed point is, however, logarithmically slow, which explains the observed nonuniversal values strongly different from -1 , see Table II. We also show there the related exponent $x_\nu = 2\alpha_\nu/(1 + \alpha_\nu)$ controlling the L scaling of the DOS, $\nu(L) \sim L^{-x_\nu}$. An

TABLE I. Critical parameters on the MIT line.

W	δ_c	ξ_M/M	α_ν	σ	$1/[2\pi(\alpha_0 - 2 + x_\nu)]$
0.3	1.64	0.72	0.015	3.3	0.70
0.5	1.22	0.73	-0.004	3.6	0.71
1.0	0.73	0.41	-0.025	2.9	0.44
2.0	0.33	0.45	-0.09	2.7	0.45
3.0	0.22	0.42	-0.11	2.6	0.40

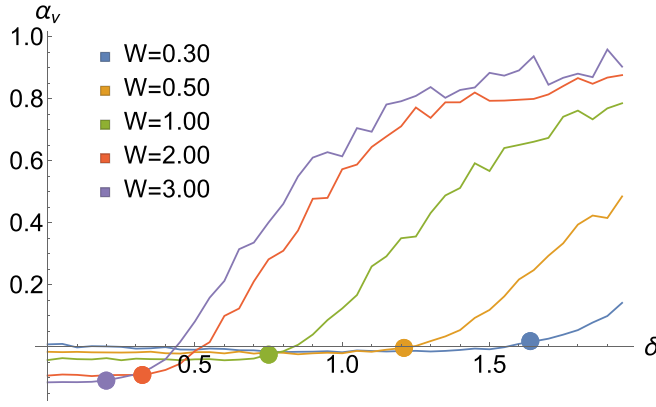


FIG. 4. Exponent $\alpha_v(W, \delta)$ of the DOS scaling, $\nu(\epsilon) \propto \epsilon^{\alpha_v}$ across the MIT at $W = 0.3, 0.5, 1, 2, 3$. Positions of the MIT critical points $\delta_c(W)$ and the corresponding values $\alpha_v(W, \delta_c(W))$ are marked by dots.

apparent non-universality is observed also at criticality, $\delta = \delta_c$, see Table I; it is analogous to the corresponding property of critical ξ_M/M (discussed above) and σ . When the system is driven into the localized phase by increasing δ , we observe a power-law behavior with an exponent α_v growing and becoming positive, in consistency with previous findings [6,7].

Conductivity. We have further studied the conductivity $\sigma(L)$ at the transition and deep in the metallic phase. For this purpose, we evaluated the conductance $g(L, M)$ (measured in units of e^2/h) of a wide sample (width M considerably exceeding the length L) using the KWANT software package [50], see the SM [49] for details. The conductivity is then obtained as $\sigma(L) = \pi g(L, M)L/M$. In the metallic phase, $\sigma(L)$ for sufficiently large L is independent on L ; the corresponding values for $\delta = 0$ are given in Table II. The L independence of $\sigma(L)$ holds also at criticality, $\delta = \delta_c$; these values are presented in Table I.

Multifractality. Moments of critical eigenfunctions exhibit multifractality, $L^2 \langle |\psi(\mathbf{r})|^{2q} \rangle \sim L^{-\Delta_q}$. Equivalently, one can study multifractality of the local DOS, $\langle \nu^q(\mathbf{r}) \rangle \sim L^{-x_q}$; the two sets of exponents are related via $x_q = \Delta_q + qx_v$. For a chiral class (bipartite lattice), one can also define moments involving wave functions on nearby sites \mathbf{r} and \mathbf{r}' belonging to different sublattices: $L^2 \langle |\psi(\mathbf{r})|^{2q} |\psi(\mathbf{r}')|^{2q'} \rangle \sim L^{-\Delta_{q,q'}}$ and $\langle \nu^q(\mathbf{r}) \nu^{q'}(\mathbf{r}') \rangle \sim L^{-x_{q,q'}}$ with $x_{q,q'} = \Delta_{q,q'} + (q+q')x_v$. In the metallic phase, the multifractal exponents can be obtained in one-loop approximation controllable for large σ . In particular,

TABLE II. Properties of the metallic phase ($\delta = 0$, various W 's). Exponents α_v and x_v of the DOS scaling, the conductivity σ from transport calculation, and couplings b , σ_1 , and κ_1 from a one-loop parabolic fit to the multifractality spectrum.

W	α_v	x_v	σ	b	σ_1	κ_1
0.3	~ -0.001	~ -0.002	48.6	0.022	41.5	~ 4
0.5	-0.005	-0.01	25.8	0.036	27.8	7.7
1.0	-0.017	-0.035	9.8	0.10	9.1	2.8
2.0	-0.10	-0.22	4.4	0.24	4.2	3.2
3.0	-0.12	-0.27	3.6	0.30	3.3	2.4

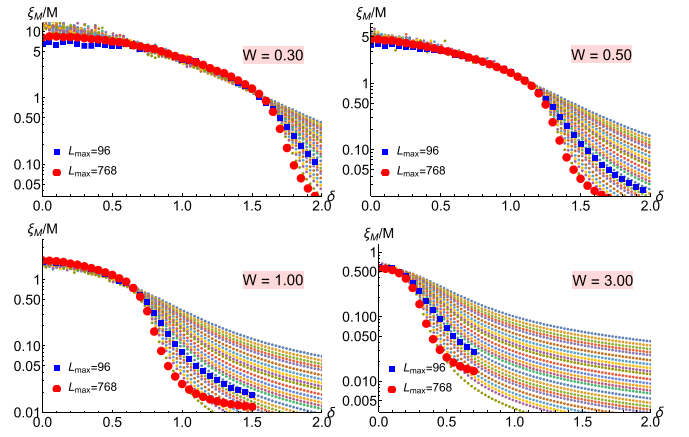


FIG. 5. Small symbols: ratio ξ_M/M from transfer-matrix analysis of a quasi-1D system with $W = 0.3, 0.5, 1$, and 3 (cf. Fig. 2). Large symbols: $1/[2\pi(\alpha_0 - 2 + x_v)]$ obtained by multifractal analysis of a 2D system with $L \leq 96$ (blue) and $L \leq 768$ (red). The relation (8) is fulfilled in the metallic phase and at criticality, see also Table I.

one-loop results for x_q and for sublattice-symmetric exponents $x_{q/2,q/2}$ read

$$x_q \simeq bq(1-q) + x_v q^2; \quad \Delta_q \simeq (b - x_v)q(1-q), \quad (6)$$

$$x_{q/2,q/2} \simeq bq(1-q/2), \quad (7)$$

with $b = 1/\sigma$ and $x_v = -\kappa/\sigma^2$. Our numerical results for the exponents Δ_q and $x_{q/2,q/2}$ in the metallic phase and at the MIT are presented in the SM [49]. In the metallic phase, the data are well described by the one-loop form (6) and (7). The corresponding one-loop fit parameters b , $\sigma_1 = 1/b$, and κ_1 are shown in Table II. We emphasize an excellent agreement between σ_1 and Landauer conductivity σ .

At the MIT, the numerically obtained multifractality spectra deviate strongly from the parabolic form, which indicates violation (at least, partial) of the conformal invariance as was also found for other 2D Anderson-transition points [51–53]. Furthermore, parameters of the multifractal spectra turn out to vary substantially along the critical line, which is another manifestation of the apparent nonuniversality discussed above.

Quasi-1D to 2D conformal mapping. An exponential map establishes a correspondence between quasi-1D (infinite cylinder) and 2D (complex plane) geometries. Under the assumption of invariance of the critical theory under this conformal transformation, one can derive [54] a relation (generalizing an earlier result of Ref. [55]),

$$M/\xi_M = 2\pi(\alpha_0 - 2 + x_v), \quad (8)$$

where $\alpha_0 = dx_q/dq|_{q=0}$. As shown in Fig. 5 and in Table I, this relation indeed holds with a very good accuracy in our class-AIII model both in the metallic phase and at the MIT.

Summary and outlook. We have numerically studied the highly peculiar MIT in a 2D tight-binding system of class AIII by supplementing a quasi-1D finite-size scaling analysis with investigation of 2D conductivity, multifractality, and the DOS. The obtained phase diagram in the parameter plane of

disorder W and staggering δ is displayed in Fig. 3. Our findings agree with the σ -model RG theory with vortices driving a transition to the insulating phase [8], yielding the flow shown in Fig. 1. We find $\nu = 1.55 \pm 0.1$ for the localization-length exponent, in agreement with the analytical estimate. Critical parameters at the MIT show an apparent nonuniversality, consistent with the analytically predicted slow renormalization along the critical line towards the ultimate $\sigma = 0$ fixed point of the MIT. Nonparabolicity of the multifractal spectrum implies a violation of conformal invariance at the MIT. At the same time, our results support invariance with respect to the

exponential conformal map between the cylinder and the plane geometries.

We foresee that future works will extend this investigation to (i) other models (e.g., on the hexagonal lattice) that are expected to provide access to strong-randomness fixed point of the MIT, (ii) other chiral classes (BDI and CII), (iii) closely related non-Hermitian ATs, and (iv) generalized multifractality in the chiral classes.

Acknowledgment. J.F.K. and A.D.M. acknowledge support by the Deutsche Forschungsgemeinschaft (DFG) via Grant No. MI 658/14-1.

-
- [1] F. Evers and A. D. Mirlin, Anderson transitions, *Rev. Mod. Phys.* **80**, 1355 (2008).
- [2] S. Stützer, Y. Plotnik, Y. Lumer, P. Titum, N. H. Lindner, M. Segev, M. C. Rechtsman, and A. Szameit, Photonic topological Anderson insulators, *Nature (London)* **560**, 461 (2018).
- [3] P. D. Antoniou and E. N. Economou, Absence of Anderson's transition in random lattices with off-diagonal disorder, *Phys. Rev. B* **16**, 3768 (1977).
- [4] R. Gade and F. Wegner, The $n = 0$ replica limit of $U(n)$ and $U(n)/SO(n)$ models, *Nucl. Phys. B* **360**, 213 (1991).
- [5] R. Gade, Anderson localization for sublattice models, *Nucl. Phys. B* **398**, 499 (1993).
- [6] O. Motrunich, K. Damle, and D. A. Huse, Particle-hole symmetric localization in two dimensions, *Phys. Rev. B* **65**, 064206 (2002).
- [7] M. Bocquet and J. T. Chalker, Network models for localization problems belonging to the chiral symmetry classes, *Phys. Rev. B* **67**, 054204 (2003).
- [8] E. J. König, P. M. Ostrovsky, I. V. Protopopov, and A. D. Mirlin, Metal-insulator transition in two-dimensional random fermion systems of chiral symmetry classes, *Phys. Rev. B* **85**, 195130 (2012).
- [9] F. J. Dyson, The dynamics of a disordered linear chain, *Phys. Rev.* **92**, 1331 (1953).
- [10] R. H. McKenzie, Exact Results for Quantum Phase Transitions In Random XY Spin Chains, *Phys. Rev. Lett.* **77**, 4804 (1996).
- [11] M. Titov, P. W. Brouwer, A. Furusaki, and C. Mudry, Fokker-planck equations and density of states in disordered quantum wires, *Phys. Rev. B* **63**, 235318 (2001).
- [12] G. Theodorou and M. H. Cohen, Extended states in a one-dimensional system with off-diagonal disorder, *Phys. Rev. B* **13**, 4597 (1976).
- [13] T. P. Eggarter and R. Riedinger, Singular behavior of tight-binding chains with off-diagonal disorder, *Phys. Rev. B* **18**, 569 (1978).
- [14] D. S. Fisher, Critical behavior of random transverse-field ising spin chains, *Phys. Rev. B* **51**, 6411 (1995).
- [15] L. Balents and M. P. A. Fisher, Delocalization transition via supersymmetry in one dimension, *Phys. Rev. B* **56**, 12970 (1997).
- [16] P. W. Brouwer, C. Mudry, B. D. Simons, and A. Altland, Delocalization in Coupled One-Dimensional Chains, *Phys. Rev. Lett.* **81**, 862 (1998).
- [17] C. Mudry, P. W. Brouwer, and A. Furusaki, Random magnetic flux problem in a quantum wire, *Phys. Rev. B* **59**, 13221 (1999).
- [18] P. Brouwer, C. Mudry, and A. Furusaki, Nonuniversality in quantum wires with off-diagonal disorder: A geometric point of view, *Nucl. Phys. B* **565**, 653 (2000).
- [19] A. Altland and R. Merkt, Spectral and transport properties of quantum wires with bond disorder, *Nucl. Phys. B* **607**, 511 (2001).
- [20] A. Altland, D. Bagrets, and A. Kamenev, Topology versus Anderson localization: Nonperturbative solutions in one dimension, *Phys. Rev. B* **91**, 085429 (2015).
- [21] J. F. Karcher, M. Sonner, and A. D. Mirlin, Disorder and interaction in chiral chains: Majoranas versus complex fermions, *Phys. Rev. B* **100**, 134207 (2019).
- [22] A. Altland and B. Simons, Field theory of the random flux model, *Nucl. Phys. B* **562**, 445 (1999).
- [23] M. Fabrizio and C. Castellani, Anderson localization in bipartite lattices, *Nucl. Phys. B* **583**, 542 (2000).
- [24] T. Fukui, Critical behavior of two-dimensional random hopping fermions with π -flux, *Nucl. Phys. B* **562**, 477 (1999).
- [25] S. Guruswamy, A. LeClair, and A. Ludwig, $gl(N|N)$ Supercurrent algebras for disordered Dirac fermions in two dimensions, *Nucl. Phys. B* **583**, 475 (2000).
- [26] C. Mudry, S. Ryu, and A. Furusaki, Density of states for the π -flux state with bipartite real random hopping only: A weak disorder approach, *Phys. Rev. B* **67**, 064202 (2003).
- [27] H. Yamada and T. Fukui, Random hopping fermions on bipartite lattices: Density of states, inverse participation ratios, and their correlations in a strong disorder regime, *Nucl. Phys. B* **679**, 632 (2004).
- [28] L. Dell'Anna, Anomalous dimensions of operators without derivatives in the non-linear σ -model for disordered bipartite lattices, *Nucl. Phys. B* **750**, 213 (2006).
- [29] Y. Hatsugai, X.-G. Wen, and M. Kohmoto, Disordered critical wave functions in random-bond models in two dimensions: Random-lattice fermions at $e = 0$ without doubling, *Phys. Rev. B* **56**, 1061 (1997).
- [30] V. Z. Cerovski, Bond-disordered Anderson model on a two-dimensional square lattice: Chiral symmetry and restoration of one-parameter scaling, *Phys. Rev. B* **62**, 12775 (2000).
- [31] A. Eilmes, R. A. Römer, and M. Schreiber, Exponents of the localization lengths in the bipartite Anderson model with off-diagonal disorder, *Physica B* **296**, 46 (2001).
- [32] A. Eilmes and R. A. Römer, Exponents of the localization length in the 2D Anderson model with off-diagonal disorder, *Phys. Status Solidi B* **241**, 2079 (2004).

- [33] P. Markoš and L. Schweitzer, Critical conductance of two-dimensional chiral systems with random magnetic flux, *Phys. Rev. B* **76**, 115318 (2007).
- [34] L. Schweitzer and P. Markoš, Disorder-driven splitting of the conductance peak at the Dirac point in graphene, *Phys. Rev. B* **78**, 205419 (2008).
- [35] P. Markoš and L. Schweitzer, Logarithmic scaling of Lyapunov exponents in disordered chiral two-dimensional lattices, *Phys. Rev. B* **81**, 205432 (2010).
- [36] L. Schweitzer and P. Markoš, Scaling at chiral quantum critical points in two dimensions, *Phys. Rev. B* **85**, 195424 (2012).
- [37] P. Markoš and L. Schweitzer, Disordered two-dimensional electron systems with chiral symmetry, *Physica B* **407**, 4016 (2012).
- [38] J. Verbaarschot, Spectrum of the QCD Dirac Operator and Chiral Random Matrix Theory, *Phys. Rev. Lett.* **72**, 2531 (1994).
- [39] M. Giordano and T. G. Kovács, Localization of Dirac fermions in finite-temperature gauge theory, *Universe* **7**, 194 (2021).
- [40] A. Rehemanjiang, M. Richter, U. Kuhl, and H.-J. Stöckmann, Microwave Realization of the Chiral Orthogonal, Unitary, and Symplectic Ensembles, *Phys. Rev. Lett.* **124**, 116801 (2020).
- [41] X. Luo, B. Xu, T. Ohtsuki, and R. Shindou, Critical behavior of Anderson transitions in three-dimensional orthogonal classes with particle-hole symmetries, *Phys. Rev. B* **101**, 020202(R) (2020).
- [42] T. Wang, T. Ohtsuki, and R. Shindou, Universality classes of the Anderson transition in the three-dimensional symmetry classes AIII, BDI, C, D, and CI, *Phys. Rev. B* **104**, 014206 (2021).
- [43] J. Feinberg and A. Zee, Non-hermitian random matrix theory: Method of hermitian reduction, *Nucl. Phys. B* **504**, 579 (1997).
- [44] Z. Gong, Y. Ashida, K. Kawabata, K. Takasan, S. Higashikawa, and M. Ueda, Topological Phases of Non-Hermitian Systems, *Phys. Rev. X* **8**, 031079 (2018).
- [45] X. Luo, Z. Xiao, K. Kawabata, T. Ohtsuki, and R. Shindou, Unifying the Anderson transitions in Hermitian and non-Hermitian systems, *Phys. Rev. Res.* **4**, L022035 (2022).
- [46] N. Hatano and D. R. Nelson, Localization Transitions in Non-Hermitian Quantum Mechanics, *Phys. Rev. Lett.* **77**, 570 (1996).
- [47] K. Kawabata and S. Ryu, Nonunitary Scaling Theory of Non-Hermitian Localization, *Phys. Rev. Lett.* **126**, 166801 (2021).
- [48] X. Luo, T. Ohtsuki, and R. Shindou, Universality Classes of the Anderson Transitions Driven by Non-Hermitian Disorder, *Phys. Rev. Lett.* **126**, 090402 (2021).
- [49] See Supplemental Material at <http://link.aps.org/supplemental/10.1103/PhysRevB.107.L020201> for details on results of numerical simulations, which includes a reference to K. Slevin and T. Ohtsuki, Critical exponent for the Anderson transition in the three-dimensional orthogonal universality class, *New J. Phys.* **16**, 015012 (2014).
- [50] C. W. Groth, M. Wimmer, A. R. Akhmerov, and X. Waintal, Kwant: A software package for quantum transport, *New J. Phys.* **16**, 063065 (2014).
- [51] J. F. Karcher, N. Charles, I. A. Gruzberg, and A. D. Mirlin, Generalized multifractality at spin quantum Hall transition, *Ann. Phys. (NY)* **435**, 168584 (2021).
- [52] J. F. Karcher, I. A. Gruzberg, and A. D. Mirlin, Generalized multifractality at the spin quantum Hall transition: Percolation mapping and pure-scaling observables, *Phys. Rev. B* **105**, 184205 (2022).
- [53] J. F. Karcher, I. A. Gruzberg, and A. D. Mirlin, Generalized multifractality at metal-insulator transitions and in metallic phases of two-dimensional disordered systems, *Phys. Rev. B* **106**, 104202 (2022).
- [54] H. Obuse, A. R. Subramaniam, A. Furusaki, I. A. Gruzberg, and A. W. W. Ludwig, Conformal invariance, multifractality, and finite-size scaling at Anderson localization transitions in two dimensions, *Phys. Rev. B* **82**, 035309 (2010).
- [55] M. Janssen, Statistics and scaling in disordered mesoscopic electron systems, *Phys. Rep.* **295**, 1 (1998).